P53/miR-34a/SIRT1 Positive Feedback Loop regulates cell proliferation and promotes cell apoptosis in the termination stage of liver regeneration.

Junhua Gong
Chongqing Medical University
Minghua Cong
Peking Union Medical College Hospital
Hao Wu
Chongqing Medical University
Menghao Wang
Chongqing Medical University
He Bai
Xi'an Medical University
Jingyuan Wang
Chongqing
Keting Que
Dianjiang People's Hospital of Chongqing
Kaiwen Zheng
Dianjiang People's Hospital of Chongqing
Wenfeng Zhang
Chongqing Medical University
Xiaoli Yang
Southwest Medical University, Sichuan
Ke Xiao
Southwest Medical University, Sichuan
Jianping Gong
Chongqing Medical University
Hanping Shi
Capital Medical University
Mingyong Miao (miaomy@163.com)
Second Military Medical University
Fangchao Yuan (846834047@qq.com)
Chongqing Medical University

Research Article

Keywords: liver regeneration, P53, miR-34a, SIRT1, HCC

Posted Date: January 20th, 2021

DOI: https://doi.org/10.21203/rs.3.rs-108116/v2

Abstract

Background The capacity of the liver to restore its architecture and function assures good prognoses of patients who suffer serious hepatic injury or cancer resection. In our study, we found that the P53/miR-34a/SIRT1 positive feedback loop has a remarkable negative regulatory effect, which is related to the termination of liver regeneration. Here, we described how P53/miR-34a/SIRT1 positive feedback loop controls liver regeneration and its possible relationship with liver cancer.

Method We performed partial hepatectomy (PH) in mice transfected with adenovirus (Ade) overexpressing P53 and adenovirus-associated virus (AAV) knock-downing miR-34a. LR was analyzed by liver weight/body weight, serum alanine aminotransferase (ALT) and aspartate aminotransferase (AST) levels and cell proliferation, and the related cellular signals were investigated. Bile acid (BA) levels during LR were analyzed by metabolomics of bile acids.

Results We found that the P53/miR-34a/SIRT1 positive feedback loop was activated in the late phase of LR. Overexpression of P53 terminated LR early and enhanced P53/miR-34a/SIRT1 positive feedback loop expression and its proapoptotic effect. Mice from the Ade-P53 group showed smaller livers and higher levels of serum ALT and AST than control mice. While knock-down of miR-34a abolished P53/miR-34a/SIRT1 positive feedback loop during LR. Mice from anti-miR-34a group showed larger livers and lower levels of PCNA-positive cells than control mice. T-β-MCA increased gradually during LR and peaked at 7 days after PH. T-β-MCA inhibited cell proliferation and promoted cell apoptosis via facilitating the P53/miR-34a/SIRT1 positive feedback loop during LR by suppressing FXR/SHP.

Conclusion The P53/miR-34a/SIRT1 positive feedback loop plays an important role in the termination of LR. Our findings shed light on the molecular and metabolic mechanisms of LR termination and provide a potential therapeutic alternative for treating P53-wild-type HCC patients.

Introduction

The astonishing regenerative capacity of the liver has been studied for decades. The capacity of the liver to restore its architecture and function assures good prognoses of patients who suffer serious hepatic injury, cancer resection, or living donor liver transplantation [1]. Thus, a better understanding of the mechanism involved in LR helps us gain insights into the cause of chronic and acute liver diseases and hepatocarcinogenesis. The complete process of LR, which includes initiation, proliferation and termination stages, requires the participation of numerous growth factors and cytokines, such as HGF, EGF, TGF-β, and TNF-α[2].

Although researchers have studied LR for decades, most of their work has focused on the initiation of LR, and little is known about the termination phase. Only a few studies have shed light on the mechanisms involved in the termination stage of LR. TGF-β secreted by hepatocytes and nonparenchymal cells has been reported to inhibit DNA synthesis in regenerating hepatocytes [3]. Other studies have shown that IL-1a is another inhibitor of liver regeneration and suppresses DNA synthesis in hepatocytes [4]. Jin J et al.

found that the cooperation between C/EBP family proteins and chromatin remodeling proteins plays important roles in the termination of LR [5]. A recent study reported that PP2Acα terminates LR in mice via the AKT/GSK3β/Cyclin D1 signaling pathway [6]. Ian Huck found that knockout of hepatocyte nuclear factor 4 alpha increased hepatocyte proliferation throughout LR and that HNF4a activation was crucial for the termination of liver regeneration in mice[7].

A previous study by Miao confirmed that miR-34a was elevated in the late phase of LR after PHx in rats and suppressed the proliferation of hepatocytes during LR[8]. Furthermore, miR-34a-induced cell death might be related to the cellular context and the miRNA targets, which modulate apoptotic cell death. miR-34a has been reported to be the direct target gene of P53[9]. Sirtuin 1 (Sirt1), which is a direct target of miR-34a, regulates the apoptosis of cells. Elevation of P53 acetylation and transcription induced by miR-34a via the suppression of Sirt1 eventually leads to apoptosis. Thus, the P53/miR-34a/SIRT1 signaling pathway functions as a positive feedback loop, in which P53 activates miR-34a, while miR-34a induces acetylation and transcription of P53 by repressing SIRT1 to modulate cell apoptosis[10]. Theoretically, if not controlled, the proapoptotic effect of the P53/miR-34a/SIRT1 positive feedback loop would be reinforced infinitely. Jiyoung Lee et al. proved that the activation of miR-34a by P53 can be inhibited by the FXR/SHP signaling pathway[11]. FXR is a known receptor of bile acids (BAs). Therefore, we intend to explore to what extent the P53/miR-34a/SIRT1 positive feedback loop is involved in the termination of LR and whether there is a putative BA functioning as a regulatory factor of the P53/miR-34a/SIRT1 pathway through the FXR/SHP signaling pathway. Moreover, unlike the uncontrollable proliferation of liver cancer cells, normal liver regeneration can be terminated in time, and the size of the liver can be accurately controlled. Therefore, the disorder of the mechanism involved in the termination of liver regeneration may be related to the occurrence and development of liver cancer. We also explored the relationship between the p53/miR-34a/SIRT1 positive feedback loop and HCC.

Materials And Methods

Experimental animals

Experiments were conducted on C57BL/6 mice (male, 19 to 22 g), which were purchased from the Experimental Animal Center of Chongqing Medical University (Chongqing, China). Prior to the experiments, standard chow and water were given to the mice ad libitum. All mice were housed in cages in a room with a controlled temperature of 23°C and humidity of 60% under a 12-h light/12-h dark cycle. The animal experiments were approved by the China Association of Laboratory Animal Care, and all efforts were made to minimize suffering. No mice were sacrificed unexpectedly during any experiments.

Adenovirus

Adenovirus (Ade) expressing green fluorescent protein (GFP) and a sequence targeting P53 was constructed by ABM (Nanjing, China). Ade-GFP was used as a control. Five days before the surgeries, mice were administered 5×10^{11} genome-equivalents of adenovirus by tail vein injection.

Adeno-associated virus-8

Adeno-associated virus-8 (AAV8) with green fluorescent protein (GFP) and a sequence targeting miR-34a was constructed by ABM (Nanjing, China), as previously described. AAV8-GFP was used as a control. Two weeks before the surgeries, mice were administered 5×10^{11} genome-equivalents of AAV8 by tail vein injection.

Experimental groups and PH

Mice were randomly divided into groups as follows:

Overexpression of P53

(1) Normal control group (NC): mice underwent sham or PH surgery (sham, n = 9 per time point; PH, n = 9 per time point); (2) Ade-GFP group: 5 days after tail vein injection of Ade-GFP, mice underwent sham or PH surgery (sham, n = 9 per time point; PH, n = 9 per time point); (3) Ade-p53 group: 5 days after tail vein injection of Ade-p53, mice underwent sham or PH surgery (sham, n = 9 per time point; PH, n = 9 per time point).

Overexpression of miR-34a

(1) Normal control group (NC): mice underwent sham or PH surgery (sham, n = 9 per time point; PH, n = 9 per time point); (2) GFP group: 2 weeks after tail vein injection of AAV8-GFP, mice underwent sham or PH surgery (sham, n = 9 per time point; PH, n = 9 per time point); (3) AAV-anti-miR-34a group: 2 weeks after tail vein injection of AAV-anti-miR-34a, mice underwent sham or PH surgery (sham, n = 9 per time point; PH, n = 9 per time point).

MCA experiment

(1) Normal diet group (ND): mice were fed a normal diet and underwent sham or PH surgery (sham, n = 9 per time point; PH, n = 9 per time point);

(2) T-β-MCA group: mice were fed normal diet and gavage with extra T-β-MCA (400 mg/kg, Steraloids, Cat# C1899-000) 1 day before PH and every 3 days after PH. Mice underwent sham or PH surgery (sham, n = 9 per time point; PH, n = 9 per time point).

Mice underwent classical PH as previously described[12]. Briefly, mice were anesthetized by intraperitoneal injection of sodium pentobarbital (50 mg/kg). Then, the left and median lobes of the liver were ligated and resected. The same surgical procedure was performed on the sham groups without conducting PH. Animals were euthanized after administration of an inhalable anesthetic (2% to 3% isoflurane) at designated times (0, 2, 3, 5, 7, 10, 14 days) after operation, and whole blood was collected via portal vein puncture. Liver tissues were quickly perfused with ice-cold phosphate-buffered saline (1×)

before they were excised and weighed. The liver/body weight ratio was calculated using the following equation: liver/body weight ratio = (remnant liver weight [g]/body weight [g]) × 100%.

Cell isolation and purification

Primary hepatocytes were isolated according to the collagenase perfusion method as previously described[13]. Briefly, mice were fully anesthetized and decontaminated, and the liver was immediately infused with buffers 1 and 2 before removal and transfer to a 100 mm cell culture plate for mechanical dissociation. The suspension (1 mL; 5×10^6 hepatocytes/mL) was dispensed into each well of 12-well culture plates and incubated at 37°C in an atmosphere of 5% CO2 for later use. The viability and purity of hepatocytes were assessed by light microscopy to ensure the presence of at least 90% hepatocytes in the suspension.

Cell transfection

Primary mouse hepatocytes were transfected with adenovirus particles with knock-in of wild-type P53 according to the manufacturer's instructions. For the control, the cells were transfected with NC or GFP in a manner identical to that used for transfection of P53. All primers were synthetized by ABM (Nanjing, China). Subsequently, the transfection efficiency was confirmed by fluorescence detection and western blot analysis. The cells were collected for further study.

Hep-3B, Huh7 and HepG2 cells (3×10^5) were seeded in each well of 6-well plates and cultured for 24h at 37 °C. The cells were then coincubated with 10 μl Lipofectamine® 2000 (Thermo Fisher Scientific, Inc., Waltham, MA, USA) and 4 μg plasmid pRFP-p53α or pRFP at 37 °C for 6 h. Subsequently, the cells were treated with fresh medium followed by an additional 24 h of incubation at 37 °C. Subsequently, the transfection efficiency was confirmed by fluorescence detection and western blot analysis. The cells were collected for further study.

Measurement of bile acid metabolites

Liver tissue was extracted from PH mice at the indicated times. Then, the samples were first suspended in sodium hydroxide (1 M) and then resuspended in methanol and pyridine. Thereafter, MCF was added and mixed by vortexing to initiate derivatization; chloroform and bicarbonate (50 mM) were then added sequentially and mixed; finally, the organic layers of samples were extracted by centrifugation (12000×g, 5 min, 24°C). The derivatized samples were transferred into glass inserts inside liquid chromatography (LC) vials after adding anhydrous sodium sulfate, and empty tubes subjected to the same process were used as negative controls. The derivatized extracts were analyzed with an ultrahigh-performance liquid chromatography (UHPLC-MS/MS) system (Agilent, 1290-6460) to quantify the differential expression of metabolites[14].

Liver histopathology

Liver tissues were fixed in 10% neutral formalin, embedded in paraffin, and then cut into 5 μm thick sections. The sections were baked at 60°C for 1 h and dehydrated with gradient ethanol and xylene. Then, the sections were stained with eosin for 30 min. After rinsing with running water for a few seconds, the sections were dehydrated with gradient ethanol and xylene and sealed with neutral gum. Histopathological changes of the liver were observed under a microscope.

Detection of liver function

Blood samples were collected from mice at the indicated time points and then centrifuged at 3000 r/min for 5 min to collect the upper translucent serum layer. Serum alanine aminotransferase (ALT) and aspartate aminotransferase (AST) levels were measured at the indicated times using a standard automatic biochemistry analyzer in the clinical biochemical laboratory.

Immunohistochemical evaluation

Liver tissues were fixed in 10% neutral formalin, embedded in paraffin, and then cut into 5 μm thick sections. The sections were dehydrated with gradient ethanol and xylene and subjected to heat-induced antigen retrieval using citrate. Then, the sections were permeabilized with 0.3% Triton for 15 min. After eliminating endogenous peroxidase activity with 3% hydrogen peroxide for 15 min, the sections were blocked with 10% fetal sheep serum for 30 min. Then, the sections were incubated with primary antibodies (1:50 dilution) overnight at 4°C. After rinsing with PBS 3 times, the sections were incubated with species-matched secondary antibodies (1:200 dilution) for 1 h at room temperature and treated with 3,3'-diaminobenzidine for 5 min at room temperature. After washing, the sections were stained with hematoxylin for 30 sec at room temperature and washed with flowing water for a few seconds. Following dehydration, the sections were sealed with neutral resin, and specific staining was visualized by light microscopy as described previously[15]. The following primary antibodies were used: anti-P53 (cat. No. Ab26; 1:50; Abcam Inc.) and anti-PCNA (cat. No. Ab92552; 1:50; Abcam Inc.).

RNA isolation and quantification

Total RNA was extracted from liver tissues using a TRIzol kit (Takara, Otsu, Japan) and was reverse transcribed into cDNA using a PrimeScript™ 1st Strand cDNA synthesis kit (Takara, Otsu, Japan). The primer sequences of miR-34a and U6 were designed and synthesized by Guangzhou RiboBio Co., LTD (Guangzhou, China). Next, qPCR assays were performed using miDETECT A Track miRNA qRT-PCR Starter Kit(RiboBio Co., LTD) and a cDNA template on an Applied Biosystems 7500 Real-time PCR system (Applied Biosystems; Thermo Fisher Scientific Inc). With U6 serving as the internal reference, the relative expression of genes was calculated using the $2^{-\Delta\Delta Ct}$ method [16].

Western blot analysis

Total proteins were extracted and denatured for 10 min at a temperature of 100°C. A total of 40 μg of protein was loaded per lane. After electrophoresis by SDS/PAGE, proteins were electrotransferred onto

polyvinylidene difluoride membranes. Then, the membranes were blocked for 1 h and incubated with primary antibodies at 4°C overnight. Primary antibodies against the following antigens were used: P53 (cat. No. Ab26; 1:1000; Abcam Inc.), Ace-P53 (cat. No. 2570S; 1:1000; CST.), SIRT1 (cat. No. 8469S; 1:1000; CST), cleaved Caspase3 (cat. No. Ab231289; 1:1000; Abcam Inc.), P21 (cat. No. Ab188224; 1:1000; Abcam Inc.), Bax (cat. No. Ab32503; 1:1000; Abcam Inc.), NR1H4 (FXR) (cat. No. Ab187735; 1:1000; Abcam Inc.), and NR0B2 (SHP) (cat. No. Ab186874; 1:1000; Abcam Inc.). The membranes were then incubated with species-matched secondary antibodies. Protein bands were visualized using the Bio-Rad ChemiDoc XRS system (Hercules, CA). All images were analyzed using NIH ImageJ software.

Ethynyl-2'-deoxyuridine cell proliferation assays

Cell proliferation was assessed by the incorporation of 5-ethynyl-2'-deoxyuridine (BeyoClick™ EdU-488 In Vitro Imaging Kit, Cat. No. C0071S, Beyotime Biotechnology Inc.) into DNA according to the manufacturer's instructions. Briefly, hepatocytes were isolated and cultured as previously described. EdU was added to the culture at a concentration of 100 nmol/L. According to the standard formaldehyde fixation protocol, the cells were permeabilized, fixed and incubated with the reaction cocktail for 30 min. The images of stained cells were captured by fluorescence microscopy[17].

TUNEL apoptosis assays

The TUNEL reaction was performed using the one step TUNEL apoptosis assay kit-green fluorescein (Cat. No. C1086, Beyotime Biotechnology Inc.) according to the manufacturer's instructions. Briefly, liver sections were deparaffinized and dehydrated. The sections were incubated in immunostaining wash buffer (0.1% Triton X-100 in PBS) for 5 min, labeled with 50 μl of TUNEL reaction mixture and incubated at 37°C for 1 h in the dark, followed by counterstaining with DAPI. After washing, slides were mounted and observed under an immunofluorescence microscope.

Statistical analysis

Statistical analyses were conducted using SPSS 22.0 software, and all values are expressed as the mean±SD. Statistical significance of differences was calculated using t-tests for parametric data involving two groups and one-way analysis of variance with Tukey's test for multiple groups. Comparisons among datasets at different time points were analyzed by repeated measurement ANOVA. The log-rank test was used to assess the differences between the survival curves. Differences were considered statistically significant if $P<0.05$.

Results

The P53/miR-34a/SIRT1 proapoptotic pathway is activated in the termination stage of LR.

To explore the function of P53/miR-34a/SIRT1 during LR in mice, we first determined whether PH could activate the P53/miR-34a/SIRT1 positive feedback loop. P53 remarkably increased at both day 2 and day 7 after PH, while no significant change was detected in miR-34a at day 2 of PH (Fig. 1A, C). Thus, P53-

induced activation of the P53/miR-34a/SIRT1 positive feedback loop might be inhibited by certain mechanisms at day 2 after PH. The level of acetylated P53 was in accordance with miR-34a expression. SIRT1 decreased gradually from day 2 to day 7 after PH and increased thereafter (Fig. 1A, C). As LR progressed, miR-34a expression gradually increased, peaked at day 7 after PH and decreased sharply thereafter (Fig. 1B). Therefore, we postulated that the P53/miR-34a/SIRT1 positive feedback loop is activated in the late stage of PH and might stimulate LR termination.

Overexpression of wild-type P53 terminates LR and enhanced the P53/miR-34a/SIRT1 positive feedback loop during LR in vivo.

To further examine the function of the P53/miR-34a/SIRT1 positive feedback loop in LR, we performed PH on mice that received tail-vein injection of adenovirus overexpressing P53 (Figure S1). The size of regenerated livers in the Ade-P53 group was significantly smaller than that of mice in the Ade-GFP group (Fig. 2A). The liver-to-body weight ratio at day 7, day 10 and day 14 was significantly lower in the Ade-P53 group, and the liver-to-body weight ratio stopped increasing starting on day 5 in the Ade-P53 group (Fig. 2B). Then, we compared the proliferation of cells in the liver during LR, and the PCNA-positive cells were higher in the Ade-GFP group on day 2 and 3 after PH (Fig. 2C, D). We investigated the serum levels of ALT and AST, which are considered two indicators of liver damage after PH. The serum levels of ALT and AST increased immediately after surgery and then decreased gradually as the liver mass and physiological structures recovered in Ade-GFP group. However, the serum levels of ALT and AST were significantly higher and did not recover to normal in Ade-P53 mice compared with GFP mice (Fig. 2E, F). The survival rate of mice that received PH surgery decreased sharply to 50% in the Ade-P53 group (Fig. 2G). TUNEL-positive cells in liver increased in P53 group (Fig. 2H, I). When P53 was overexpressed, the P53/miR-34a/SIRT1 positive feedback loop was enhanced at 7 days after PH (Fig. 2J, K). Therefore, these data suggest that knock-in of P53 enhanced P53/miR-34a/SIRT1 positive feedback loop during LR and terminates LR early.

Knock-down of miR-34a inhibited the P53/miR-34a/SIRT1 positive feedback loop during LR and postpones LR termination in vivo.

To further examine the function of the P53/miR-34a/SIRT1 positive feedback loop in LR, we performed PH on mice that received tail-vein injection of AAV that down-regulated miR-34a (Figure S2). The size of regenerated livers in the anti-miR-34a group was significantly bigger than that of mice in the AAV-GFP group at day 7 after PH (Fig. 3A). The liver-to-body weight ratio at day 5, 7, 10 and 14 were significantly higher in the anti-miR-34a group (Fig. 3B). We next assessed cell proliferation by PCNA staining, and cell proliferation in the liver was promoted in the anti-miR-34a group at 3, 5, 7, 10 days after PH (Fig. 3C, D). TUNEL-positive cells in liver decreased sharply in anti-miR-34a group (Fig. 3E, F). When miR-34a was knocked down, the P53/miR-34a/SIRT1 positive feedback loop was down-regulated, as were the proapoptotic genes downstream (Fig. 3G, H). Therefore, these data suggest that knock-down of miR-34a abolished the P53/miR-34a/SIRT1 positive feedback loop during LR and LR could not be terminated then.

T-β-MCA enhanced the proapoptotic effect of the P53-activated P53/miR-34a/SIRT1 positive feedback loop in primary mouse hepatocytes by suppressing the FXR/SHP signaling pathway.

It has been proven that BAs participate in LR by acting as signaling molecules that activate signaling pathways [18,19]. Previous studies have confirmed a stimulatory role of BA at physiological concentrations in LR [20,21]. Here, we analyzed BAs in the regenerated liver tissue of mice. In our study, we found that there was a difference in the activation of the P53/miR-34a/SIRT1 positive feedback loop between the early and late stages of LR (Fig 1A). P53 level increased at both 2 days and 7 days after PH (Fig 1A). The miR-34a level did not increased, nether the P53/miR-34a/SIRT1 positive feedback loop were activated at 2 days after PH (Fig 1A, B). Therefore, P53 transactivation of miR-34a was inhibited in the early stage of LR. We postulated that this might be due to the change in the BA pool during LR.

We performed metabolomics of BAs during LR, which included 22 BAs in total, by UHPLC (Table S1). Among these BAs, 13 changed significantly during LR in our study (Fig 4A). The levels of 5 BAs were elevated during LR compared with the Sham group. The levels of 8 BAs decreased in the latter phase of LR. Among the top 3 BAs with the highest concentrations, T-β-MCA increased gradually during LR (Fig 4B). We observed that the level of T-β-MCA was correlated with the level of miR-34a. As LR progressed, the level of T-β-MCA gradually increased, peaked at day 7 after PH and decreased sharply thereafter (Fig 4C). Therefore, these data suggest that the P53/miR-34a/SIRT1 positive feedback loop might be manipulated by T-β-MCA.

Beta-muricholic acid (bMCA) is a major BA in rats and mice [22]. In a recent major study, Fredrik Backhed and his colleagues proved that tauro-β-muricholic acid (T-β-MCA) is a competitive and reversible FXR antagonist and that treatment with T-β-MCA reduces TCA-induced activation of the FXR/SHP signaling pathway[23]. Activating the FXR/SHP signaling pathway can inhibit the transcriptional activation of miR-34a by P53[11]. Therefore, we hypothesized that T-β-MCA is able to enhance the effect of the P53-activated P53/miR-34a/SIRT1 positive feedback loop by suppressing the FXR/SHP signaling pathway.

We transfected primary mouse hepatocytes with adenovirus carrying wild-type P53. The transfection efficiency was verified by WB and fluorescent imaging (Figure S3). In our study, TUNEL staining showed that the apoptosis of hepatocytes was enhanced by T-β-MCA (Fig 4D, E). We found that P53 overexpression activated the P53/miR-34a/SIRT1 positive feedback loop in primary mouse hepatocytes, while it was enhanced by the administration of T-β-MCA downstream of proapoptotic genes (Fig 4G-H). The FXR/SHP signaling pathway is inhibited by T-β-MCA treatment. Treatment with GW4064, an FXR/SHP signaling pathway agonist, was able to activate the FXR/SHP signaling pathway and inhibit the P53/miR-34a/SIRT1 positive feedback loop in primary mouse hepatocytes. When cells were co-incubated with T-β-MCA, the GW4064-induced activation of the FXR/SHP signaling pathway was inhibited.

T-β-MCA facilitates the P53/miR-34a/SIRT1 positive feedback loop during LR by suppressing the FXR/SHP signaling pathway in mice.

We next performed PH on mice fed a normal diet (ND) and mice fed extra T-β-MCA in sterile water by gavage. The size of regenerated livers in the T-β-MCA group was significantly smaller than that of mice in the ND group at 7 days after PH (Fig. 5A). The liver-to-body weight ratio at days 5, 7, 10 and 14 after PH was significantly lower in the T-β-MCA group (Fig. 5B). PCNA staining showed that cell proliferation was suppressed in the T-β-MCA group (Fig. 5C, D). The serum levels of ALT and AST increased immediately after surgery and then decreased gradually as the liver mass and physiological structures recovered in ND group. However, the serum levels of ALT and AST were significantly higher and did not recover to normal in T-β-MCA mice compared with ND mice (Fig. 5E, F). The survival rate of mice that received PH surgery decreased sharply to 50% in the Ade-P53 group (Fig. 5G). TUNEL-positive cells in liver increased in T-β-MCA group (Fig. 5H, I). WB showed that the effect of the P53/miR-34a/SIRT1 positive feedback loop increased, while FXR/SHP was inhibited in the T-β-MCA group (Fig. 5J, K). Therefore, these data suggest that T-β-MCA is able to facilitate the proapoptotic effect of the P53-activated P53/miR-34a/SIRT1 positive feedback loop by suppressing the FXR/SHP signaling pathway and terminate LR early in vivo.

Knock-in of wild-type P53 reinforce the P53/miR-34a/SIRT1 positive feedback loop in in P53-wild-type HepG2 cell lines.

Hepatocellular carcinoma (HCC) is a malignant tumor and the third leading cause of cancer-related mortality[24]. Both LR and HCC are characterized by high cell proliferation, but there are significant differences between the two. The unlimited proliferation of HCC cells lacks a termination mechanism, while during LR, cell proliferation can be terminated, and liver mass is precisely regulated. Due to TP53 mutations, the P53 response pathway is frequently deficient in HCC patients[25,26]. Thus, we hypothesized that P53/miR-34a/SIRT1 fails to function during HCC due to the loss or mutation of P53.

Accordingly, we evaluated the functions and expression of the P53/miR-34a/SIRT1 positive feedback loop in vitro. To elucidate the effects of the P53/miR-34a/SIRT1 positive feedback loop on cell apoptosis and proliferation in vitro, we investigated liver cancer cells with different endogenous P53 expression levels, HepG2 (P53-wt), Hep3B (P53-de) and Huh7 (P53-mut) and overexpressed wild-type P53 with a plasmid[27] (Figure S4 A). The transfection efficiency was verified by WB and fluorescent imaging (Figure S4 B C). Only two CAs function as FXR antagonists, T-β-MCA in mice and ursodeoxycholic acid (UDCA) in human[28,29]. In our experiment, we test the other FXR antagonist UDCA's effect on P53/miR-34a/SIRT1 positive feedback loop in human liver cancer cell as well[30].

The P53/miR-34a/SIRT1 positive feedback loop was detected in P53-wild-type HepG2 cells (Fig 6A-C). Administration of UDCA alone increased P53/miR-34a/SIRT1 positive feedback loop expression and its down-stream targets (Fig 6A-C). Overexpression of wild-type P53 enhanced P53/miR-34a/SIRT1 positive feedback loop expression and its pro-apoptotic effect in HepG2 cells and could be facilitated even more by administration of UDCA (Fig 6A-C). Overexpression of wild-type P53 increased TUNEL-positive cells and inhibited proliferation of HepG2 cells, and UDCA could improve its effect (Fig 6D, E).

Knock-in of wild-type P53 restored the P53/miR-34a/SIRT1 positive feedback in P53-mutated Huh-7 cell line.

The P53/miR-34a/SIRT1 positive feedback loop was absent in P53-mutated Huh7 cells, while overexpression of wild-type P53 in Hep3B cells restored the P53/miR-34a/SIRT1 positive feedback loop and could be further enhanced by administration of UDCA (Fig 7A-C). Additionally, the FXR/SHP signaling pathway was inhibited by administration of UDCA in Huh7 cells (Fig 7A-C). Overexpression of wild-type P53 increased apoptosis and inhibited proliferation of Huh7 cells, and UDCA could improve its effect (Fig 7D, E).

Knock-in of wild-type P53 restored the P53/miR-34a/SIRT1 positive feedback in P53-deficient Hep-3B cell lines.

The P53/miR-34a/SIRT1 positive feedback loop does not exist in P53-deficient Hep3B cells. Overexpression of wild-type P53 in Hep3B cells restored the P53/miR-34a/SIRT1 positive feedback loop, which could be further enhanced by administration of UDCA (Fig 8A-C). Additionally, the FXR/SHP signaling pathway was inhibited by administration of UDCA in Hep3B cells (Fig 8A-C). Overexpression of wild-type P53 increased apoptosis and inhibited proliferation of Hep3B cells, and UDCA could improve its effect (Fig 8D, E).

Discussion

The liver is extremely vulnerable to physical and chemical damage. LR protects the liver by helping the liver recover from such damage. However, the exact mechanisms underlying the termination stage of LR after PH remain unclear. In this study, we demonstrated that the P53/miR-34a/SIRT1 positive feedback loop was significantly activated in the late stage of LR. Furthermore, overexpression of P53 increased apoptosis of hepatocytes during LR and ended LR beforehand, while knock-down of miR-34a abolished P53/miR-34a/SIRT1 positive feedback loop during LR and suppressed LR termination (Fig 2, 3). Here, we propose a new mechanism that regulates the termination of LR to enrich the understanding of the underlying regulatory mechanism. As the P53/miR-34a/SIRT1 positive feedback loop has been reported to be involved in blocking cell proliferation and inducing cell apoptosis in numerous cell lines and diseases, our research will provide new insights into the study of P53/miR-34a/SIRT1 in both LR and tumorigenesis.

Yamakuchi and his colleagues overexpressed miR-34a and found decreased SIRT1 expression, resulting in increased acetylated P53 levels and increased levels of P53 targets such as p21 and PUMA[10]. This is how the P53/miR-34a/SIRT1 positive feedback loop functions. It has been shown that the P53/miR-34a/SIRT1 positive feedback loop is activated according to disease severity in human non-alcoholic fatty liver disease (NAFLD), and several antitumor drugs could activate the P53/miR-34a/SIRT1 positive feedback loop in cancer cell lines to induce the apoptosis of cancer cells[31,32]. Duarte M. S. Ferreira et al. demonstrated that P53/miR-34a/SIRT1 activated by JNK1/c-Jun contributed to cell death caused by deoxycholic acid in rats[33]. In our study, the P53/miR-34a/SIRT1 positive feedback loop was activated in the late stage of LR, and its proapoptotic and antiproliferative effects could be necessary to terminate LR. Serum ALT and AST levels in mice after PH did not recover to normal in mice overexpressing P53, which

might be due to liver regeneration in mice overexpressing P53 being terminated earlier than under normal conditions. Overexpression of P53 intensified the effect of the P53/miR-34a/SIRT1 positive feedback loop in the termination stage of LR at 7 days after PH (Fig 2K). Our findings suggest that the P53/miR-34a/SIRT1 positive feedback loop is activated during the termination stage of LR rather than the initiation or proliferation stage. Although there was an increase in P53, it failed to stimulate the P53/miR-34a/SIRT1 positive feedback loop in the early phase of LR (Fig 1A). Thus, there might be a certain mechanism that controls the activation of the P53/miR-34a/SIRT1 positive feedback loop. Meanwhile, knocked-down of miR-34a suppressed the P53/miR-34a/SIRT1 positive feedback loop and its effect (Fig. 3G, H). LR became infinitely and could not be terminated during the first 14 days after PH (Fig. 3B). These data suggest P53/miR-34a/SIRT1 positive feedback loop is essential for LR termination.

In our study, we found that total BAs increased in the early phase of LR and then decreased in the termination stage of LR, with a gradual increase in the proportion of T-β-MCA over total BA (Fig 4B, C). Sama I. Sayin et al. identified T-β-MCA as an FXR antagonist that inhibited the FXR/SHP signaling pathway[23]. Our study showed that T-β-MCA suppressed the FXR/SHP signaling pathway and amplified the proapoptotic effects of P53-induced activation of the P53/miR-34a/SIRT1 positive feedback loop both in vitro and in vivo.

TP53 mutations are commonly found in HCC patients. Previous research showed that TP53 had the highest prevalence of protein-altering mutations in HCC[34,35]. Several studies have shown that tumor drugs can suppress the proliferation of liver cancer cells by activating the P53/miR-34a/SIRT1 positive feedback loop[36,32]. In our study, we show that the P53/miR-34a/SIRT1 positive feedback loop is deficient in the P53-deficient Hep3B and P53-mutated Huh7 cell lines. The P53 level is higher in the P53-mutated Huh7 cell line than in the HepG2 cell line, while the P53/miR-34a/SIRT1 positive feedback loop is not activated. After knock-in of wild-type P53, the P53/miR-34a/SIRT1 positive feedback loop was restored and further enhanced by administration of UDCA through suppressing FXR/SHP in all cell lines. Administration of UDCA alone in the wild-type P53 HepG2 cell line promoted the P53/miR-34a/SIRT1 positive feedback loop. Thus, deficiency in the P53/miR-34a/SIRT1 positive feedback loop induced by the mutation or loss of P53 might be the cause of HCC tumorigenesis and development. Additionally, UDCA or other alternative FXR antagonist could be a potential therapeutic target for HCC patients with wild-type P53 expression.

Conclusion

In summary, a P53/miR-34a/SIRT1 positive feedback loop exists and is activated in the termination of LR. The effect of the P53/miR-34a/SIRT1 positive feedback loop is regulated by T-β-MCA/UDCA through the FXR/SHP signaling pathway, and the mechanism is summarized in the diagram (Graphical Abstract). These findings may provide new insight into the treatment of chronic liver diseases, liver transplantation, and liver malignancy, especially for HCC patients with wild-type P53 expression.

Abbreviations

ALT: alanine transaminase; AST: aspertate aminotransferase; AAV: adenovirus associated virus; Ade: adenovirus; BA: bile acid; FXR: farnesoid x receptor; GFP: green fluorescent protein; HCC: hepatocellular carcinoma; IHC: immunohistochemistry; LR: liver regeneration; MCA: muricholic acid; T-β-MCA: tauro-β-muricholic acid; PH: partial hepatectomy; RFP: red fluorescent protein; SHP: small heterodimer partner; TUNEL: TdT-mediated dUTP nick end labeling; UDCA: ursodeoxycholic acid; UHPLC: ultrahigh-performance liquid chromatography.

Declarations

Ethics approval and consent to participate

Ethical reviews of animal experiment were approved by the ethics committee of the Second Affiliated Hospital of Chongqing Medical university and all animals' care and experimental protocols were in line with the Animal Management Rules of the Ministry of Health of the People's Republic of China.

Consent for publication

The study was conducted in accordance with the protocol approved by the Declaration of Helsinki and the guidelines of the Ethics Review Committee of the Second Affiliated Hospital of Chongqing Medical University

Availability of data and materials

The data sets used and/or analyzed during the current study are available from the corresponding author on reasonable request.

Competing interests

All of the authors declare that there are no competing interests.

Funding

This study was supported by grants from the National Natural Science Foundation of China (NSFC: No. 81971880 awarded to GJP; No. 81570569 awarded to MMY and No. 81672888 awarded to HPS) administered by the the National Natural Science Fund Committee.

Authors' contributions

FCY and MYM designed the study. JHG and MHC carried out the animal experiments. HW and MHW performed the cell experiments. XLY, HB and JYW conducted the molecular cloning and staining experiments. KX, KWZ and WFZ analyzed the data. JHG and MHC wrote the manuscript, HPS and JPG revised the manuscript. All authors have read and approved the final version of this manuscript.

Acknowledgements

The preprint of this paper had been uploaded on researchsquare. The preprint should not be considered conclusive, used to inform clinical practice, or referenced by the media as validated information.

References

1. Jia C (2011) Advances in the regulation of liver regeneration. Expert Rev Gastroenterol Hepatol 5 (1):105-121. doi:10.1586/egh.10.87
2. Miyajima A, Tanaka M, Itoh T (2014) Stem/progenitor cells in liver development, homeostasis, regeneration, and reprogramming. Cell Stem Cell 14 (5):561-574. doi:10.1016/j.stem.2014.04.010
3. Kogure K, Zhang YQ, Maeshima A, Suzuki K, Kuwano H, Kojima I (2000) The role of activin and transforming growth factor-beta in the regulation of organ mass in the rat liver. Hepatology 31 (4):916-921. doi:10.1053/he.2000.6100
4. Boulton R, Woodman A, Calnan D, Selden C, Tam F, Hodgson H (1997) Nonparenchymal cells from regenerating rat liver generate interleukin-1alpha and -1beta: a mechanism of negative regulation of hepatocyte proliferation. Hepatology 26 (1):49-58. doi:10.1053/jhep.1997.v26.pm0009214451
5. Jin J, Hong IH, Lewis K, Iakova P, Breaux M, Jiang Y, Sullivan E, Jawanmardi N, Timchenko L, Timchenko NA (2015) Cooperation of C/EBP family proteins and chromatin remodeling proteins is essential for termination of liver regeneration. Hepatology 61 (1):315-325. doi:10.1002/hep.27295
6. Lai SS, Zhao DD, Cao P, Lu K, Luo OY, Chen WB, Liu J, Jiang EZ, Yu ZH, Lee G, Li J, Yu DC, Xu XJ, Zhu MS, Gao X, Li CJ, Xue B (2016) PP2Acalpha positively regulates the termination of liver regeneration in mice through the AKT/GSK3beta/Cyclin D1 pathway. J Hepatol 64 (2):352-360. doi:10.1016/j.jhep.2015.09.025
7. Huck I, Gunewardena S, Espanol-Suner R, Willenbring H, Apte U (2019) Hepatocyte Nuclear Factor 4 Alpha Activation Is Essential for Termination of Liver Regeneration in Mice. Hepatology 70 (2):666-681. doi:10.1002/hep.30405
8. Chen H, Sun Y, Dong R, Yang S, Pan C, Xiang D, Miao M, Jiao B (2011) Mir-34a is upregulated during liver regeneration in rats and is associated with the suppression of hepatocyte proliferation. PloS one 6 (5):e20238-e20238. doi:10.1371/journal.pone.0020238
9. Chang TC, Wentzel EA, Kent OA, Ramachandran K, Mullendore M, Lee KH, Feldmann G, Yamakuchi M, Ferlito M, Lowenstein CJ, Arking DE, Beer MA, Maitra A, Mendell JT (2007) Transactivation of miR-34a by p53 broadly influences gene expression and promotes apoptosis. Mol Cell 26 (5):745-752. doi:10.1016/j.molcel.2007.05.010
10. Yamakuchi M, Ferlito M, Lowenstein CJ (2008) miR-34a repression of SIRT1 regulates apoptosis. Proc Natl Acad Sci U S A 105 (36):13421-13426. doi:10.1073/pnas.0801613105
11. Lee J, Padhye A, Sharma A, Song G, Miao J, Mo YY, Wang L, Kemper JK (2010) A pathway involving farnesoid X receptor and small heterodimer partner positively regulates hepatic sirtuin 1 levels via microRNA-34a inhibition. J Biol Chem 285 (17):12604-12611. doi:10.1074/jbc.M109.094524

12. Wang M, Yuan F, Bai H, Zhang J, Wu H, Zheng K, Zhang W, Miao M, Gong J (2019) SHMT2 Promotes Liver Regeneration Through Glycine-activated Akt/mTOR Pathway. Transplantation 103 (7):e188-e197. doi:10.1097/tp.0000000000002747
13. Georgila K, Gounis M, Havaki S, Gorgoulis VG, Eliopoulos AG (2020) mTORC1-dependent protein synthesis and autophagy uncouple in the regulation of Apolipoprotein A-I expression. Metabolism 105:154186. doi:10.1016/j.metabol.2020.154186
14. Kakiyama G, Muto A, Takei H, Nittono H, Murai T, Kurosawa T, Hofmann AF, Pandak WM, Bajaj JS (2014) A simple and accurate HPLC method for fecal bile acid profile in healthy and cirrhotic subjects: validation by GC-MS and LC-MS. J Lipid Res 55 (5):978-990. doi:10.1194/jlr.D047506
15. Xie Y, Zhao D, Dong P, Lai L (2018) Macrophage-targeting Fasudil treatment protects liver from the ischemia/reperfusion injury by promoting M2 macrophage polarization. Biosci Rep. doi:10.1042/BSR20171734
16. Arocho A, Chen B, Ladanyi M, Pan Q (2006) Validation of the 2-DeltaDeltaCt calculation as an alternate method of data analysis for quantitative PCR of BCR-ABL P210 transcripts. Diagn Mol Pathol 15 (1):56-61. doi:10.1097/00019606-200603000-00009
17. Zhong H, Wu H, Bai H, Wang M, Wen J, Gong J, Miao M, Yuan F (2019) Panax notoginseng saponins promote liver regeneration through activation of the PI3K/AKT/mTOR cell proliferation pathway and upregulation of the AKT/Bad cell survival pathway in mice. BMC Complement Altern Med 19 (1):122. doi:10.1186/s12906-019-2536-2
18. Drudi Metalli V, Mancino MG, Mancino A, Torrice A, Gatto M, Attili AF, Alpini G, Alvaro D (2007) Bile salts regulate proliferation and apoptosis of liver cells by modulating the IGF1 system. Dig Liver Dis 39 (7):654-662. doi:10.1016/j.dld.2007.03.008
19. Fan M, Wang X, Xu G, Yan Q, Huang W (2015) Bile acid signaling and liver regeneration. Biochim Biophys Acta 1849 (2):196-200. doi:10.1016/j.bbagrm.2014.05.021
20. Monte MJ, El-Mir MY, Sainz GR, Bravo P, Marin JJ (1997) Bile acid secretion during synchronized rat liver regeneration. Biochim Biophys Acta 1362 (1):56-66
21. Ding L, Yang Y, Qu Y, Yang T, Wang K, Liu W, Xia W (2015) Bile acid promotes liver regeneration via farnesoid X receptor signaling pathways in rats. Mol Med Rep 11 (6):4431-4437. doi:10.3892/mmr.2015.3270
22. Hofmann AF, Hagey LR, Krasowski MD (2010) Bile salts of vertebrates: structural variation and possible evolutionary significance. J Lipid Res 51 (2):226-246. doi:10.1194/jlr.R000042
23. Sayin SI, Wahlstrom A, Felin J, Jantti S, Marschall HU, Bamberg K, Angelin B, Hyotylainen T, Oresic M, Backhed F (2013) Gut microbiota regulates bile acid metabolism by reducing the levels of tauro-beta-muricholic acid, a naturally occurring FXR antagonist. Cell Metab 17 (2):225-235. doi:10.1016/j.cmet.2013.01.003
24. Gan L, Liu Z, Sun C (2018) Obesity linking to hepatocellular carcinoma: A global view. Biochim Biophys Acta Rev Cancer 1869 (2):97-102. doi:10.1016/j.bbcan.2017.12.006

25. Olivier M, Hussain SP, Caron de Fromentel C, Hainaut P, Harris CC (2004) TP53 mutation spectra and load: a tool for generating hypotheses on the etiology of cancer. IARC Sci Publ (157):247-270
26. Hussain SP, Schwank J, Staib F, Wang XW, Harris CC (2007) TP53 mutations and hepatocellular carcinoma: insights into the etiology and pathogenesis of liver cancer. Oncogene 26 (15):2166-2176. doi:10.1038/sj.onc.1210279
27. Kanno S-i, Kurauchi K, Tomizawa A, Yomogida S, Ishikawa M (2015) Pifithrin-alpha has a p53-independent cytoprotective effect on docosahexaenoic acid-induced cytotoxicity in human hepatocellular carcinoma HepG2 cells. Toxicology Letters 232 (2):393-402. doi:https://doi.org/10.1016/j.toxlet.2014.11.016
28. Wahlstrom A, Sayin SI, Marschall HU, Backhed F (2016) Intestinal Crosstalk between Bile Acids and Microbiota and Its Impact on Host Metabolism. Cell Metab 24 (1):41-50. doi:10.1016/j.cmet.2016.05.005
29. de Aguiar Vallim TQ, Tarling EJ, Edwards PA (2013) Pleiotropic roles of bile acids in metabolism. Cell Metab 17 (5):657-669. doi:10.1016/j.cmet.2013.03.013
30. Buryova H, Chalupsky K, Zbodakova O, Kanchev I, Jirouskova M, Gregor M, Sedlacek R (2013) Liver protective effect of ursodeoxycholic acid includes regulation of ADAM17 activity. BMC Gastroenterol 13:155. doi:10.1186/1471-230X-13-155
31. Audrito V, Vaisitti T, Rossi D, Gottardi D, D'Arena G, Laurenti L, Gaidano G, Malavasi F, Deaglio S (2011) Nicotinamide blocks proliferation and induces apoptosis of chronic lymphocytic leukemia cells through activation of the p53/miR-34a/SIRT1 tumor suppressor network. Cancer Res 71 (13):4473-4483. doi:10.1158/0008-5472.CAN-10-4452
32. Lou G, Liu Y, Wu S, Xue J, Yang F, Fu H, Zheng M, Chen Z (2015) The p53/miR-34a/SIRT1 Positive Feedback Loop in Quercetin-Induced Apoptosis. Cell Physiol Biochem 35 (6):2192-2202. doi:10.1159/000374024
33. Ferreira DM, Afonso MB, Rodrigues PM, Simao AL, Pereira DM, Borralho PM, Rodrigues CM, Castro RE (2014) c-Jun N-terminal kinase 1/c-Jun activation of the p53/microRNA 34a/sirtuin 1 pathway contributes to apoptosis induced by deoxycholic acid in rat liver. Mol Cell Biol 34 (6):1100-1120. doi:10.1128/MCB.00420-13
34. Neuveut C, Wei Y, Buendia MA (2010) Mechanisms of HBV-related hepatocarcinogenesis. J Hepatol 52 (4):594-604. doi:10.1016/j.jhep.2009.10.033
35. Kan Z, Zheng H, Liu X, Li S, Barber TD, Gong Z, Gao H, Hao K, Willard MD, Xu J, Hauptschein R, Rejto PA, Fernandez J, Wang G, Zhang Q, Wang B, Chen R, Wang J, Lee NP, Zhou W, Lin Z, Peng Z, Yi K, Chen S, Li L, Fan X, Yang J, Ye R, Ju J, Wang K, Estrella H, Deng S, Wei P, Qiu M, Wulur IH, Liu J, Ehsani ME, Zhang C, Loboda A, Sung WK, Aggarwal A, Poon RT, Fan ST, Wang J, Hardwick J, Reinhard C, Dai H, Li Y, Luk JM, Mao M (2013) Whole-genome sequencing identifies recurrent mutations in hepatocellular carcinoma. Genome Res 23 (9):1422-1433. doi:10.1101/gr.154492.113
36. Xia C, Shui L, Lou G, Ye B, Zhu W, Wang J, Wu S, Xu X, Mao L, Xu W, Chen Z, Liu Y, Zheng M (2017) 0404 inhibits hepatocellular carcinoma through a p53/miR-34a/SIRT1 positive feedback loop. Sci

Rep 7 (1):4396. doi:10.1038/s41598-017-04487-x

Figures

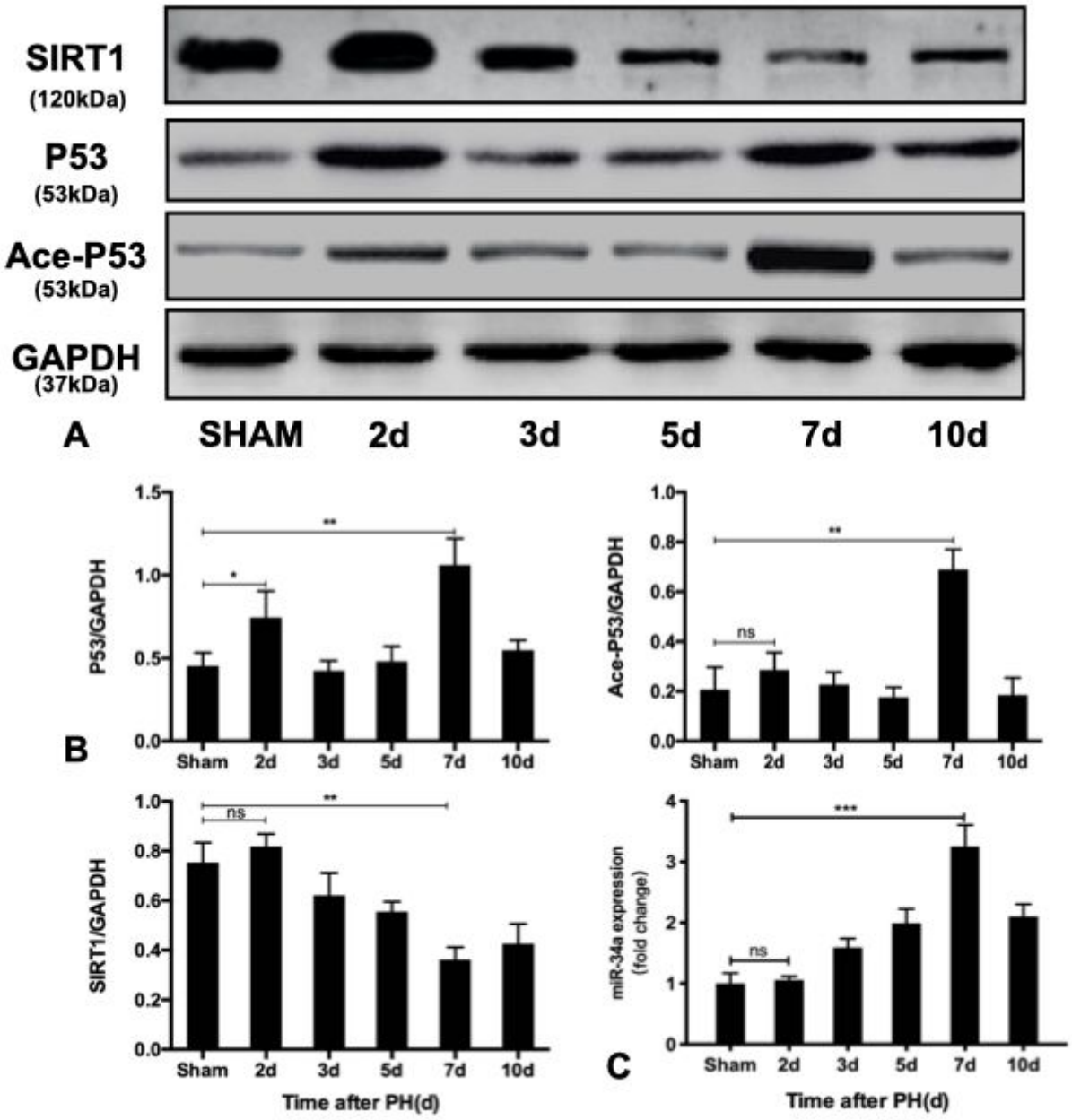

Figure 1

P53/miR-34a/SIRT1 positive feedback loop expression during LR. (A) Protein expression of the P53/miR-34a/SIRT1 positive feedback loop during LR progression was analyzed via western blot. (B) Quantification of hepatic P53, Ace-P53, and SIRT1 expression at the indicated time points after PH by WB. (C) Quantification of hepatic miR-34a expression at the indicated time points after PH by qPCR. (ns: not significant, $p>0.05$; *, $p<0.05$; **, $p<0.01$; ***, $p<0.001$).

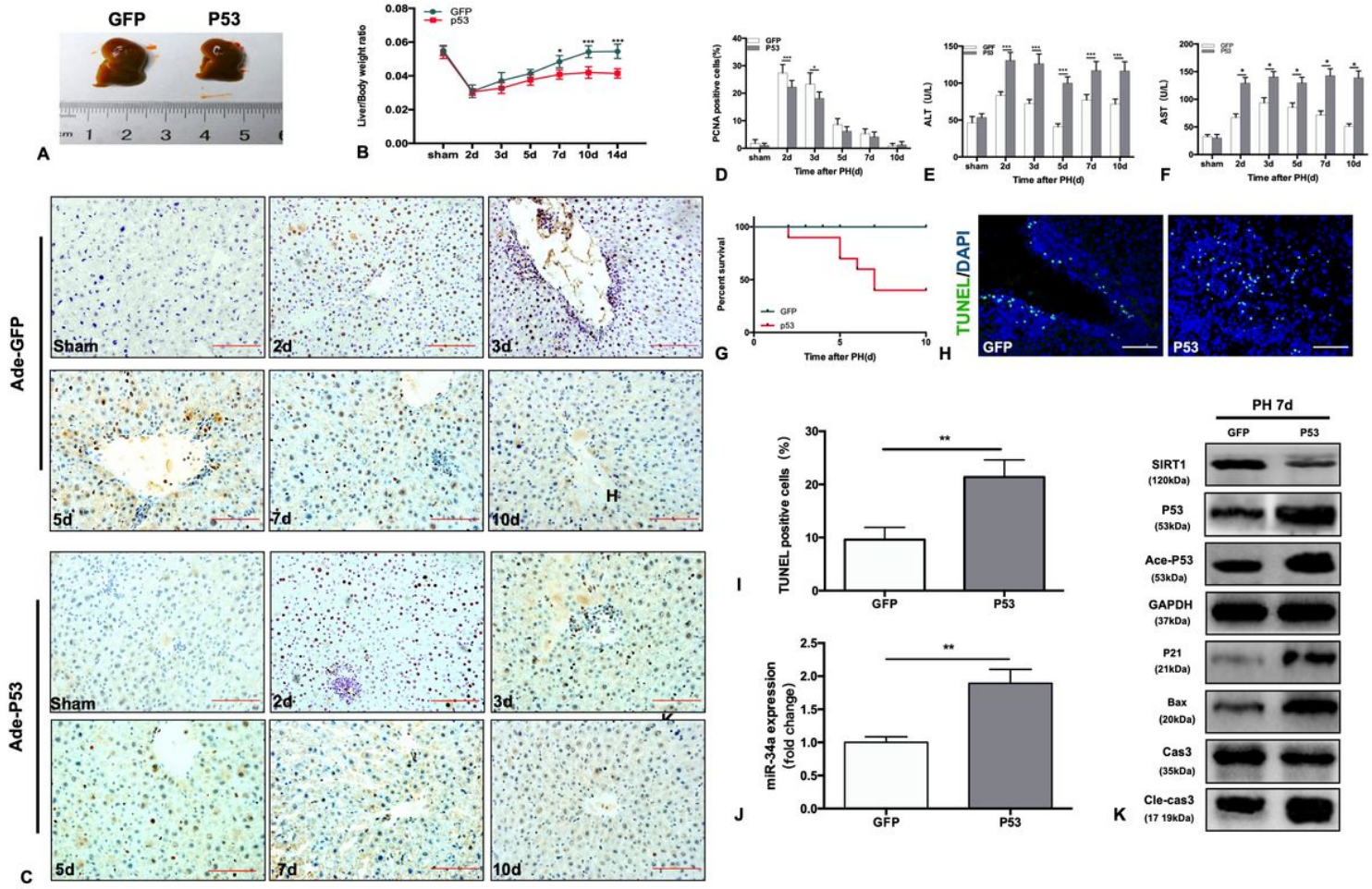

Figure 2

Overexpression of wild-type P53 terminates LR and activates the P53/miR-34a/SIRT1 positive feedback loop early during LR. (A) Representative livers from mice at 7 days after PH between Ade-GFP and Ade-P53 mice. (B) Liver weight relative to body weight at the indicated time points after PH. (C) Representative images of PCNA staining at the indicated time points after PH from the Ade-GFP and Ade-P53 groups (magnification: ×200, scale bars represent 50 μm). (D) Quantification of PCNA-positive cells in the liver at the indicated time points after PH. (E, F) Serum AST and ALT levels in Ade-GFP and Ade-P53 mice after PH. (G) Survival rate of mice that underwent PH from the Ade-GFP and Ade-P53 groups. (H) Representative images of TUNEL staining at day 7 after PH in liver tissue (magnification: ×400). (I)Quantification of TUNEL-positive cells in the liver at day 7 after PH. (J) Quantification of hepatic miR-34a expression between Ade-GFP and Ade-P53 mice at day 7 after PH by qPCR. (K) Protein expression of P53/miR-34a/SIRT1 positive feedback loop genes between Ade-GFP and Ade-P53 mice day 7 after PH. (*, p<0.05; **, p<0.01; ***, p<0.001).

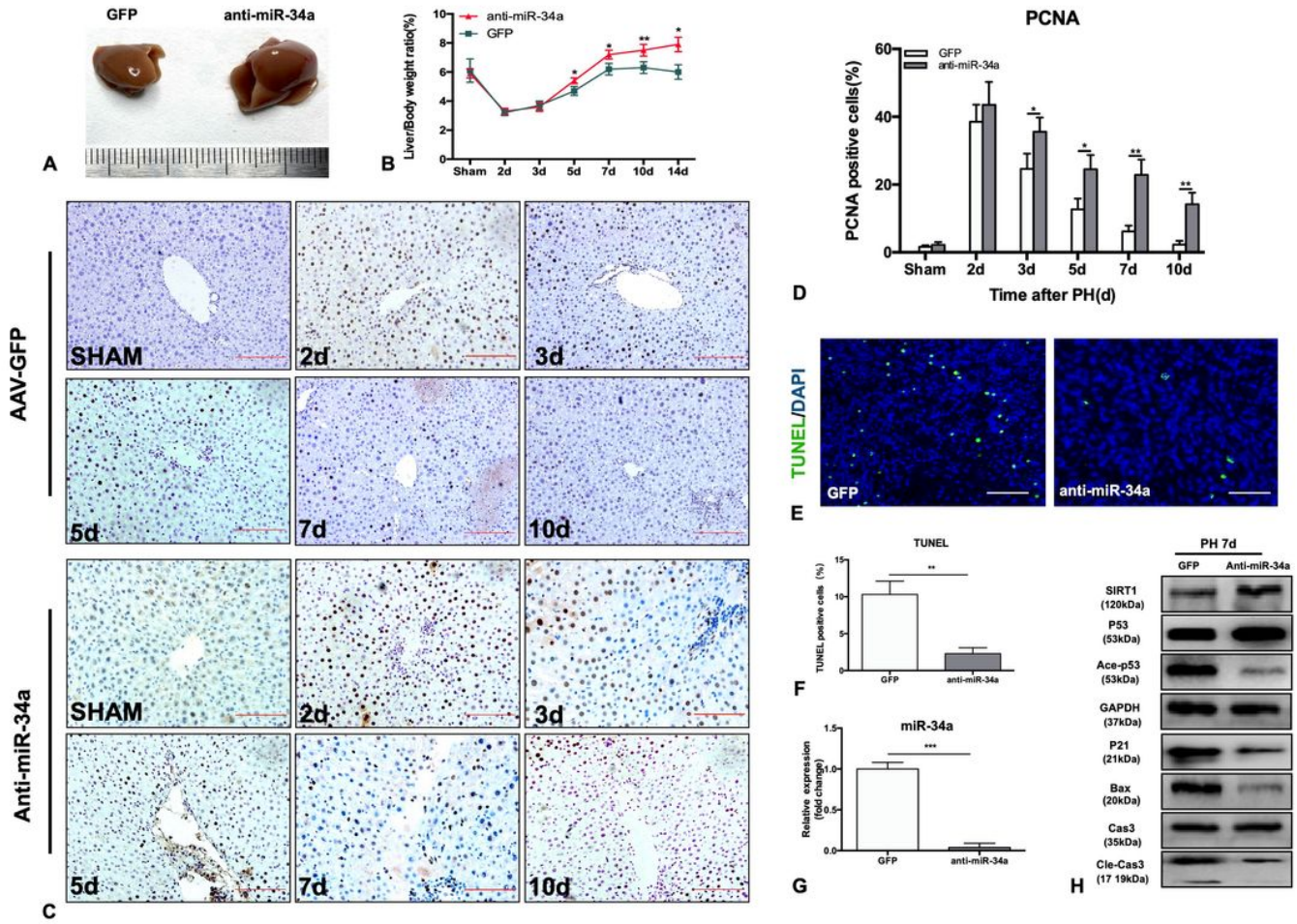

Figure 3

Knock-down of miR-34a suppresses the P53/miR-34a/SIRT1 positive feedback loop early during LR. (A) Representative livers from mice at 7 days after PH between AAV-GFP and AAV-anti-miR-34a mice. (B) Liver weight relative to body weight at the indicated time points after PH. (C)Representative images of PCNA staining at the indicated time points after PH in the GFP and anti-miR-34a groups (magnification: ×200, scale bars represent 50 μm).(D) Quantification of PCNA-positive cells in the liver at the indicated time points after PH.(E) Representative images of TUNEL staining at day 7 after PH in liver tissue(magnification: ×400). (F)Quantification of TUNEL-positive cells in the liver at day 7 after PH. (G)Protein expression of P53/miR-34a/SIRT1 positive feedback loop genes between AAV-GFP and AAV-miR-34a mice at day 7 after PH. (H) Quantification of hepatic miR-34a expression between AAV-GFP and AAV-miR-34a mice at day 7 after PH by qPCR. (*, p<0.05; **, p<0.01; ***, p<0.001).

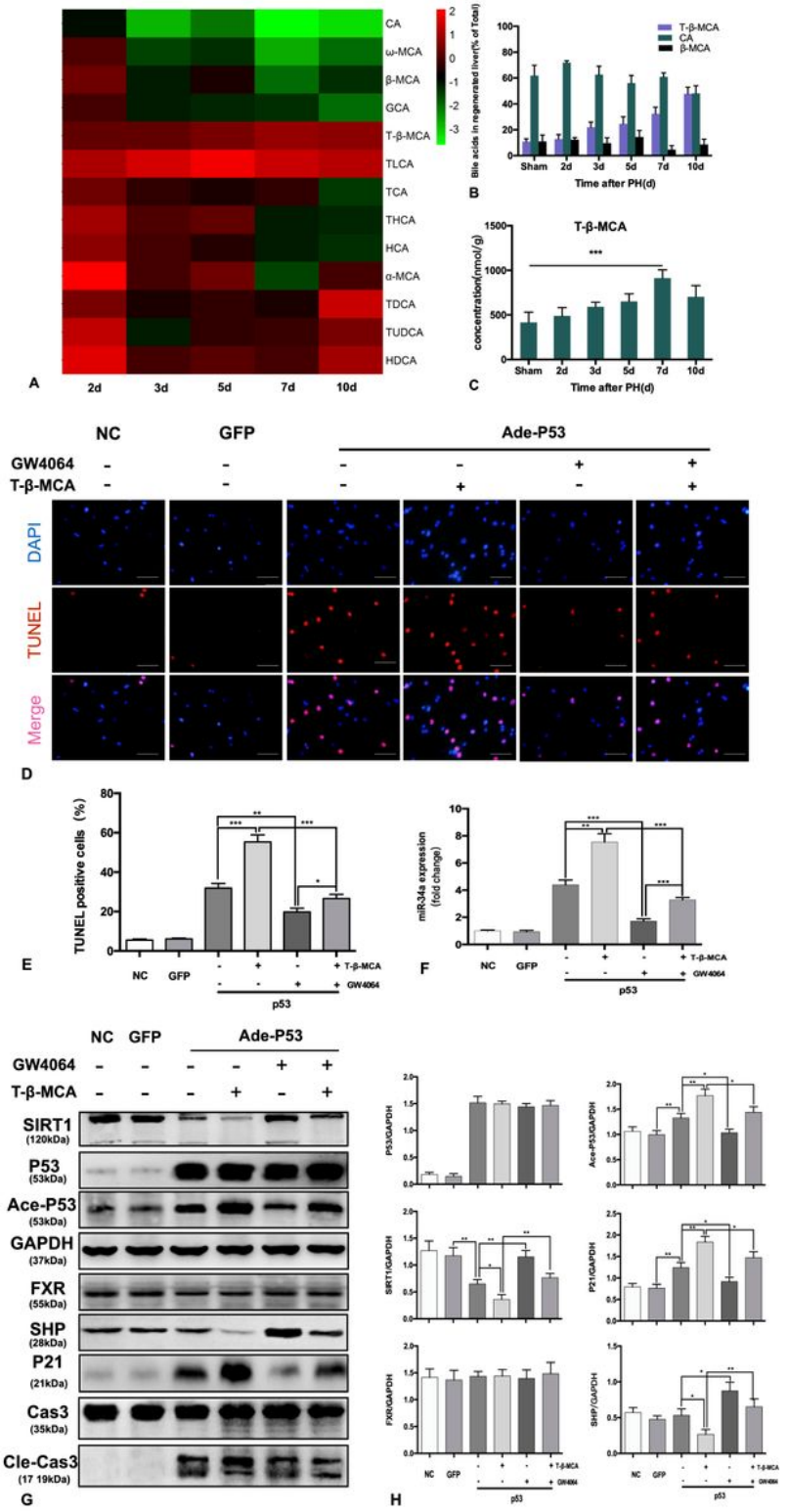

Figure 4

T-β-MCA enhanced the proapoptotic effect of the P53-activated P53/miR-34a/SIRT1 positive feedback loop by suppressing the FXR/SHP signaling pathway in vitro. (A) Heatmap of changed Bas during LR. (B) Percentage of the top 3 BAs at the indicated time points after PH. (C) Concentration of T-β-MCA at the indicated time points after PH. (D)TUNEL staining of primary hepatocytes after knock-in of P53 with/without administration of T-β-MCA and GW4064(magnification: × 400, Scale bars represent 50 μm).

(E)Quantification of TUNEL-positive cells after knock-in of P53 with/without administration of T-β-MCA and GW4064.(F)Quantification of hepatic miR-34a expression in mouse primary hepatocytes after knock-in of P53 with/without administration of T-β-MCA and GW4064 by qPCR.(G)Protein expression of P53/miR-34a/SIRT1 positive feedback loop genes and FXR/SHP signaling after knock-in of P53 with/without administration of T-β-MCA and GW4064. Cells were pretreated with/without 100 μM T-β-MCA or 1 μM GW4064 for 12 h. (H) Quantification of P53, Ace-P53, SIRT1, P21, FXR, and SHP protein expression by WB. (ns: p>0.05; *, p<0.05; **, p<0.01; ***, p<0.001).

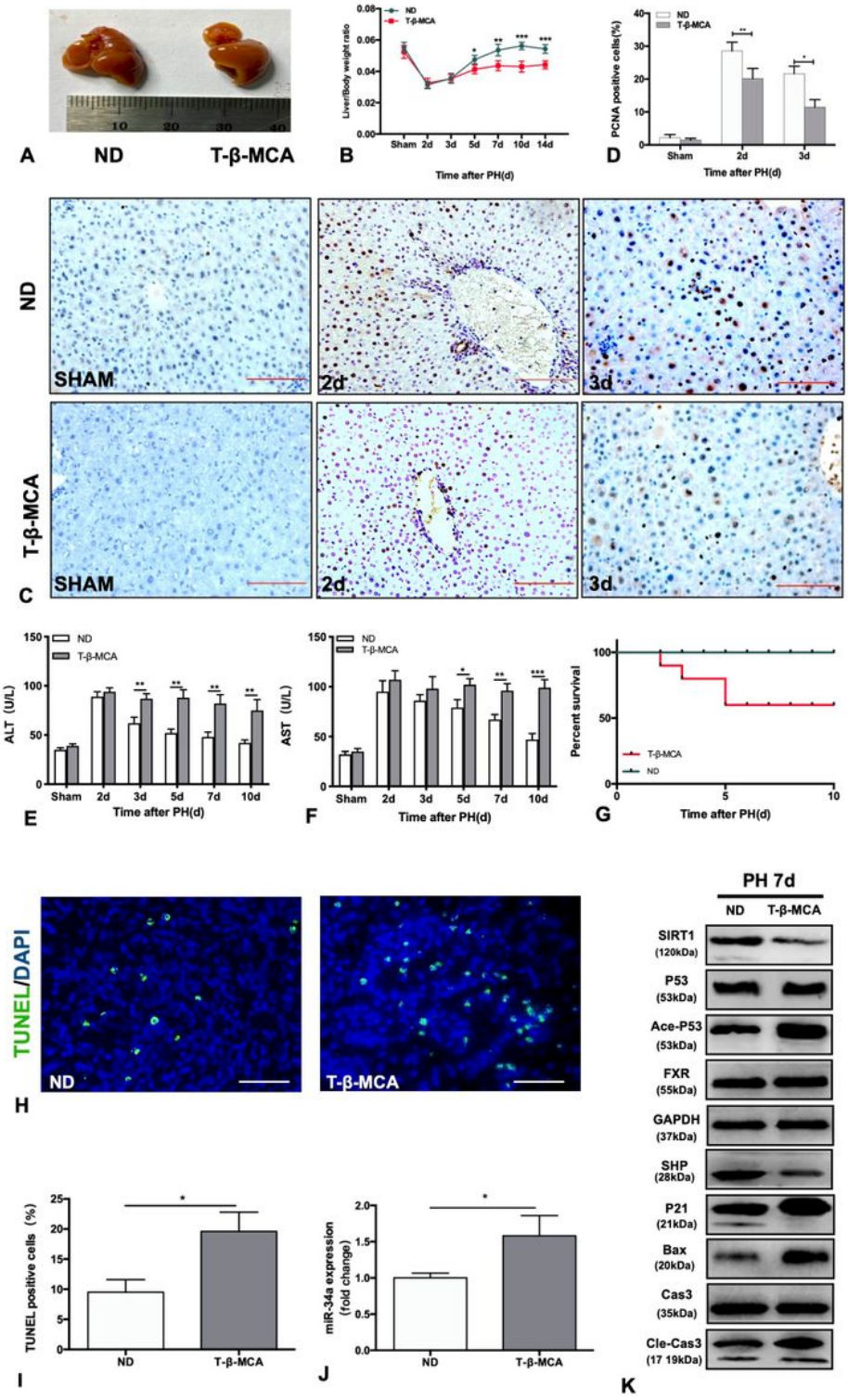

Figure 5

T-β-MCA facilitates the P53/miR-34a/SIRT1 positive feedback loop during LR by suppressing the FXR/SHP signaling pathway in vivo. (A) Representative livers from mice at 7 days after PH between ND and T-β-MCA mice. Mice in the T-β-MCA group were administered T-β-MCA (400 mg/kg) by gavage 1 day before PH and every 3 days after PH (B) Liver weight relative to body weight at the indicated time points after PH.(C) Representative images of PCNA staining at the indicated time points after PH from the ND and T-β-MCA groups. (magnification: × 200, Scale bars represent 50 μm). (D) Quantification of PCNA-positive cells in the liver at the indicated time points after PH. (E, F) Serum AST and ALT levels in mice from the ND and MCA groups after PH. (G) Survival rate of mice that underwent PH from the ND and T-β-MCA groups. (H) Representative images of TUNEL staining at day 7 after PH in liver tissue (magnification: ×400). (I)Quantification of TUNEL-positive cells in the liver at day 7 after PH. (J)Quantification of hepatic miR-34a expression in mice with/without administration of T-β-MCA. (K) Protein expression of P53/miR-34a/SIRT1 positive feedback loop genes and FXR/SHP signaling with/without administration of T-β-MCA. *, $p<0.05$. (ns: not significant, $p>0.05$; *, $p<0.05$; **, $p<0.01$; ***, $p<0.001$).

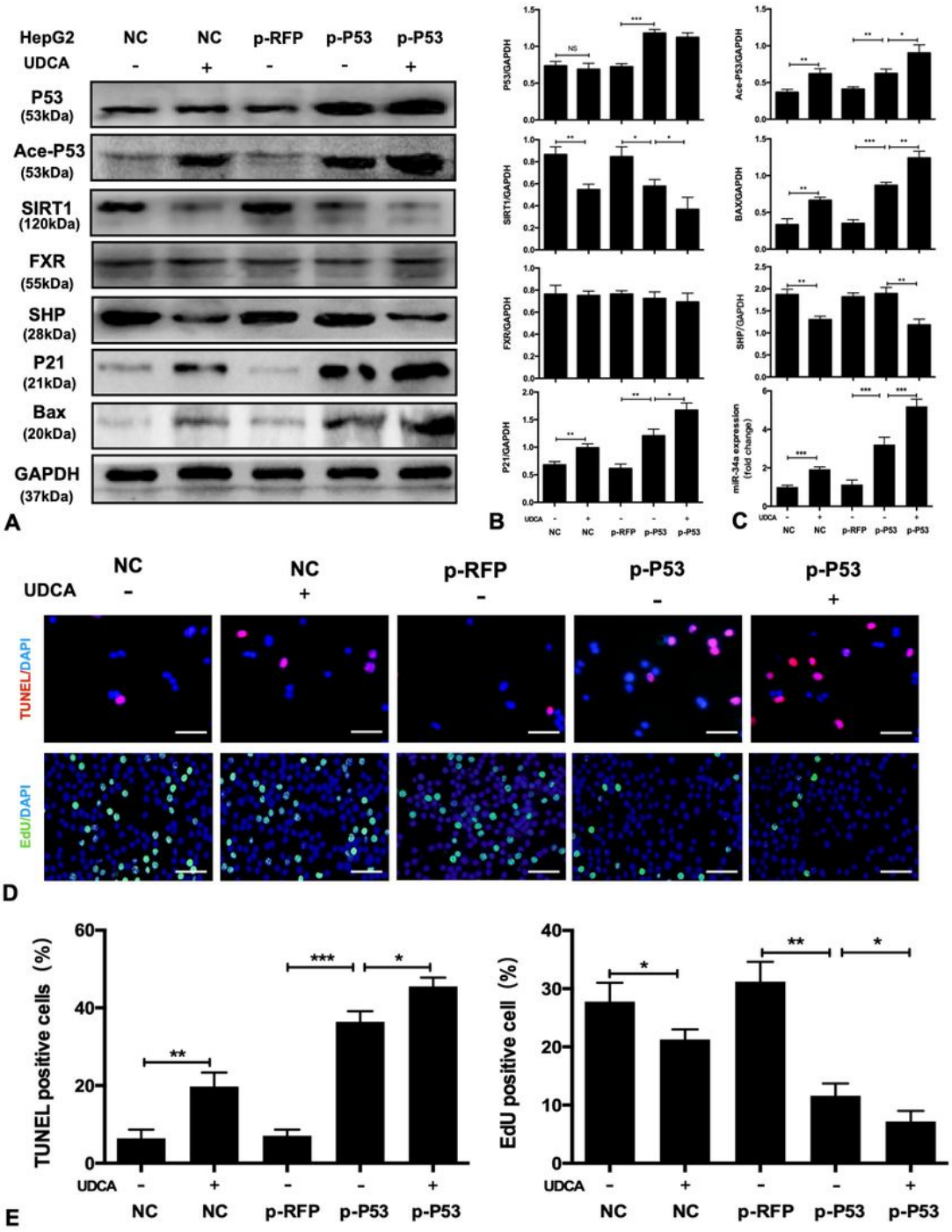

Figure 6

Knock-in of wild-type P53 reinforce the P53/miR-34a/SIRT1 positive feedback loop in P53-wild-type HepG2 cell lines. (A) Protein expression of P53/miR-34a/SIRT1 positive feedback loop genes and FXR/SHP signaling after knock-in of wild-type P53 with/without administration of UDCA in P53-wild-type HepG2 cells. Cells were pretreated with/without 200 μM UDCA for 2 h before the experiment. (B) Quantification of P53, Ace-P53, SIRT1, P21, BAX, FXR, and SHP protein expression by WB. (C)

Quantification of miR-34a expression in P53-wild-type HepG2 cells after knock-in of wild-type P53 with/without administration of UDCA. (D) TUNEL and EdU staining of P53-wild-type HepG2 cells after knock-in of wild-type P53 with/without administration of UDCA. (E) Quantification of TUNEL-positive and EdU-positive HepG2 cells after knock-in of wild-type P53 with/without administration of UDCA. (ns: not significant, p>0.05; *, p<0.05; **, p<0.01; ***, p<0.001).

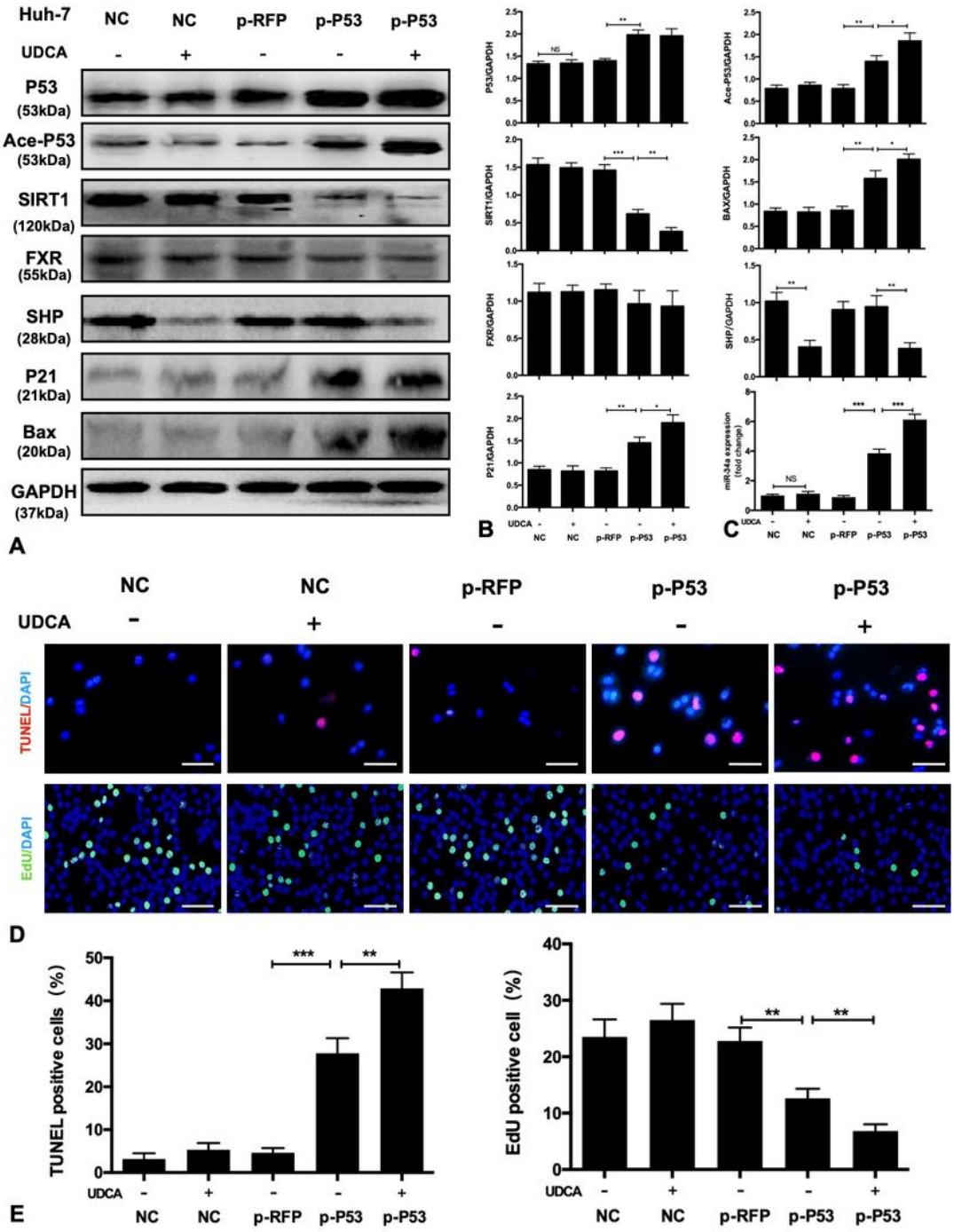

Figure 7

Knock-in of wild-type P53 restored the P53/miR-34a/SIRT1 positive feedback in P53-mutated Huh-7 cell line.(A) Protein expression of P53/miR-34a/SIRT1 positive feedback loop genes and FXR/SHP signaling after knock-in of wild-type P53 with/without administration of UDCA in P53-mutated Huh-7 cells. Cells were pretreated with/without 200 μM UDCA for 2 h before the experiment. (B) Quantification of P53, Ace-P53, SIRT1, P21, BAX, FXR, and SHP protein expression by WB. (C) Quantification of miR-34a expression in P53-mutated Huh-7 cells after knock-in of wild-type P53 with/without administration of UDCA. (D) TUNEL and EdU staining of P53-mutated Huh-7 cells after knock-in of wild-type P53 with/without administration of UDCA (magnification: × 400, Scale bars represent 50 μm). (E) Quantification of TUNEL-positive and EdU-positive Huh-7 cells after knock-in of wild-type P53 with/without administration of UDCA. (ns: not significant, $p>0.05$; *, $p<0.05$; **, $p<0.01$; ***, $p<0.001$).

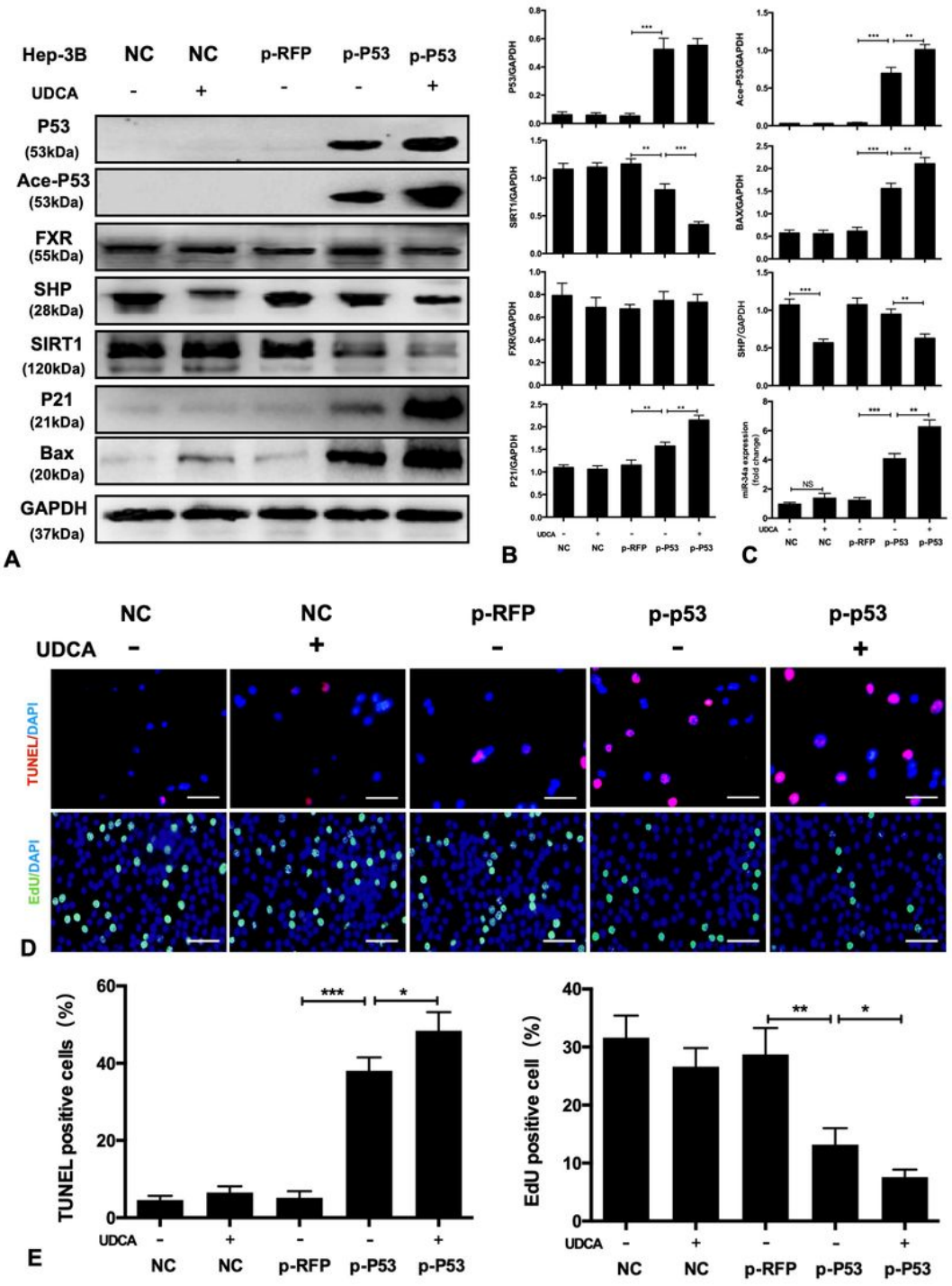

Figure 8

Knock-in of wild-type P53 restored the P53/miR-34a/SIRT1 positive feedback in P53-deficient Hep-3B cell lines. (A) Protein expression of P53/miR-34a/SIRT1 positive feedback loop genes and FXR/SHP signaling after knock-in of wild-type P53 with/without administration of UDCA in P53-deficient Hep3B cells. Cells were pretreated with/without 200 μM UDCA for 2 h before the experiment. (B) Quantification of P53, Ace-P53, SIRT1, P21, BAX, FXR, and SHP protein expression by WB (C) Quantification of miR-34a expression

in P53-deficient Hep3B cells after knock-in of wild-type P53 with/without administration of UDCA. (D) TUNEL and EdU staining of P53-deficient Hep3B cells after knock-in of wild-type P53 with/without administration of UDCA (magnification: × 400, Scale bars represent 50 μm). (E) Quantification of TUNEL-positive and EdU-positive Hep3B cells after knock-in of wild-type P53 with/without administration of UDCA. (ns: not significant, $p>0.05$; *, $p<0.05$; **, $p<0.01$; ***, $p<0.001$).

Supplementary Files

This is a list of supplementary files associated with this preprint. Click to download.

- figureS1.jpg
- figs2.jp2
- FigS3.jp2
- FigS4.jp2
- SupplementaryCB.docx
- GraphicalAbstract.png